

Transport signatures of dominant spin-orbit coupling in two-dimensional materials

Valentina Brosco,¹ Lara Benfatto,¹ Emmanuele Cappelluti,¹ and Claudio Grimaldi²

¹*ISC-CNR and Department of Physics, Sapienza University of Rome, P.le A. Moro 2, 00185 Rome, Italy*

²*Laboratory of Physics of Complex Matter, Ecole Polytechnique
Fédérale de Lausanne, Station 3, CH-1015 Lausanne, Switzerland*

We investigate the transport properties of the Rashba model in the strong spin-orbit coupling regime. We show that as soon as the energy associated with SO interaction overcomes the Fermi energy and it becomes the largest energy scale in the system the dc conductivity computed by Kubo formula shows substantial deviations from usual Drude transport law, with a strong density dependence of the mobility. This result is accurately reproduced by an approximate analytical expression that could be tested in the experiments, providing a powerful tool to asses the strength of the SO coupling in two-dimensional materials.

PACS numbers: 71.70.Ej, 72.10.-d

The interplay between spin and orbital degrees of freedom may have profound consequences on the properties of matter [1–3]. Under appropriate conditions, spin-orbit (SO) interaction governs spin relaxation [4–6], it leads to spin-polarized currents [7–9], and it induces new topological phases [10–13]. Enabling the control of spins by electrical means, spin-orbit interaction also plays a crucial role in the implementation of spin-based electronics devices [14]. Of particular interest in these regards are emerging classes of two-dimensional materials, like surface alloys [15–20], layered bismuth telluro-halides [21–24], HgTe quantum wells [25] and interfaces between complex oxides [26–38] where the lack of inversion symmetry induces a Rashba SO coupling [1, 39] tunable [18, 20, 24, 33–38] and considerably stronger than what found in traditional III-V semiconductor heterostructures [40, 41].

Due to their low dimensionality these systems provide the ideal playground to explore different doping regimes. Specifically, they can be driven towards a “dominant spin-orbit (DSO) regime”, achieved when the SO energy, E_0 , overcomes the Fermi energy becoming the dominant energy scale in the system. It has been shown that this regime changes the nature of disorder-induced localization [42], gives rise to unconventional spin relaxation [43] and it may strongly enhance superconductivity [44]. In the present Letter we demonstrate that it also leads to strongly unconventional charge transport properties. To this aim we compute the dc charge conductivity, σ_{dc} , in a fully conserving approach, in the presence of short-ranged impurities for arbitrary SO coupling strengths. Differently from previous studies, encompassing spin Hall effect [2, 3, 45–48] and charge magnetotransport [3, 49–51], we focus on the DSO regime and we show that, for densities below a certain threshold, $n \leq n_0 \propto E_0$, σ_{dc} acquires a non-trivial dependence on the density itself, obeying the approximate formula:

$$\sigma_{DSO} \simeq \frac{e^2 \tau_0}{m} \frac{n^2}{2n_0} \left(1 + \frac{n^2}{n_0^2} \right), \quad n \leq n_0, \quad (1)$$

where m is the effective mass of the carriers, and τ_0 is the transport scattering time in the opposite ($n \geq n_0$) regime where a standard Drude-like behavior, $\sigma_{dc} = ne^2 \tau_0 / m$, is recovered. The non-linearity of σ_{dc}^{DSO} as a function of n , reflected in a strong charge-density dependence of the carrier mobility, provides a clear trademark for the DSO regime and it can be employed to get an unbiased estimate of the underlying Rashba parameters n_0 and E_0 . Beside being relevant for all materials with strong SO coupling, our results may shed new light on the deviations from Drude transport laws observed in $\text{LaAlO}_3/\text{SrTiO}_3$ interfaces [30–33], although these materials have an electronic structure more complex than the Rashba model investigated here.

In spite of its simplicity, Eq.(1) stems from two concomitant effects: the suppression of the single-particle scattering time $\tau(n) \sim \tau_0(n/n_0)$ for $n \leq n_0$, due to the non-constant electronic density of states (DOS) [44], and a non-vanishing renormalization of the “anomalous” current vertex operator, responsible for the factor in brackets in Eq. (1). As we show below, these quantum effects are only partly captured by the semiclassical Boltzmann approach, limiting its applicability in the DSO regime.

We consider a two-dimensional electron gas confined to the plane (x, y) in the presence of Rashba SO interaction and disorder generated by static impurities. The system is described by the following Hamiltonian

$$H = \int d\mathbf{r} \Psi^\dagger(\mathbf{r}) \left[\frac{p^2}{2m} + \alpha \hat{z} \cdot (\mathbf{p} \times \vec{\sigma}) + V_{\text{imp}}(\mathbf{r}) \right] \Psi(\mathbf{r}), \quad (2)$$

where \mathcal{V} is the volume of the system, $V_{\text{imp}}(\mathbf{r})$ is the disorder potential, α is the SO coupling, $\vec{\sigma}$ is the vector of Pauli matrices and $\Psi(\mathbf{r})$ and $\Psi^\dagger(\mathbf{r})$ are spinor fields which respectively create and destroy electrons at position \mathbf{r} . Here we limit ourselves to the simplest case of Gaussian random disorder with “white noise” correlations, namely $\langle V_{\text{imp}}(\mathbf{r}) V_{\text{imp}}(\mathbf{r}') \rangle_{\text{imp}} = n_{\text{imp}} v_{\text{imp}}^2 \delta(\mathbf{r} - \mathbf{r}')$ where v_{imp} and n_{imp} denote respectively the scattering strength and the impurity density.

In the absence of impurities, Eq. (2) gives an electronic spectrum consisting of two bands with helicity $s = \pm 1$ and dispersion $E_p^s = (p + sp_0)^2/(2m) - E_0$ with $p_0 = m\alpha$ and $E_0 = m\alpha^2/2$. When the chemical potential, μ , crosses the point $\mu = 0$ where the two bands touch, the structure of the Fermi surface changes. As shown in Fig.1, for $\mu > 0$, the Fermi surface consists of two circles corresponding to different helicities, while for $\mu < 0$, the Fermi level crosses only the negative-helicity band. The value $\mu = 0$ separates also two different regimes in the DOS: for $\mu > 0$ the DOS at the Fermi level is constant, $N_0 = m/(\pi\hbar^2)$, while for $\mu < 0$ it displays [44] a van Hove singularity. Consequently, in the two cases, the electronic density, n , is related to μ and E_0 as follows

$$n \simeq \begin{cases} N_0(E_F + E_0) & \mu > 0 \\ 2N_0\sqrt{E_F E_0} & \mu < 0 \end{cases} \quad (3)$$

where we introduced the “Fermi energy” $E_F = \mu + E_0$. From the above equation we can estimate the critical density n_0 where the system enters the DSO regime as $n_0 \equiv n(\mu = 0) = 2mE_0/(\pi\hbar^2)$.

In the presence of impurities, within self-consistent Born approximation (SCBA), the amount and strength of disorder and the different transport regimes, can be roughly quantified using the quasi-particle relaxation rate [52] at zero SO coupling, $\Gamma_0 = m n_{\text{imp}} v_{\text{imp}}^2/(2\hbar^2)$. Most theoretical works on the spin-Hall effect and on magnetotransport consider the high-density limit, $\mu \gg 0$, for either “weak” ($E_0 \ll \Gamma_0$) or “strong” ($E_0 \gg \Gamma_0$) SO coupling [3, 4, 6, 51]. Here we focus on the strong SO coupling case, $E_0 \gg \Gamma_0$, and we relax the high-density assumption allowing for both $\mu > 0$ and $\mu < 0$ (DSO regime).

The SCBA retarded Green’s function is given by the following matrix in spin space [47, 52],

$$G^R(\mathbf{p}, \omega) = \frac{1}{2} \sum_{s=\pm} [\mathbb{I} + s(\hat{p} \times \boldsymbol{\sigma})] g_s^R(p, \omega), \quad (4)$$

where \mathbb{I} is the identity matrix, $\hat{p} = \mathbf{p}/|\mathbf{p}|$ and $g_s(p, \omega)$ denotes the Green function of electrons with helicity s ,

$$g_s^R(p, \omega) = [\omega - E_p^s + \mu - \Sigma^R(\omega)]^{-1}. \quad (5)$$

The self-energy $\Sigma^R(\omega)$ is spin and momentum independent and it satisfies the self-consistent equation $\Sigma^R(\phi) = n_{\text{imp}} v_{\text{imp}}^2 \sum_{\mathbf{p}, s} g_s^R(p, \phi)$ [52]. At zero frequency its imaginary part defines the elastic scattering rate of quasiparticles, $\Gamma = -\text{Im}[\Sigma^R(0)] = (n_{\text{imp}} v_{\text{imp}}^2 \pi/\mathcal{V}) \sum_{\mathbf{p}, s} \mathcal{A}_s(p)$, where $\mathcal{A}_s(p) = -(1/\pi) \text{Im} g_s^R(p, \phi = 0)$ is the spectral function of each helicity band, so that Γ scales as the DOS at the Fermi level. In the “weak-disorder approximation” (WDA), valid for $\Gamma \ll E_F$, we can approximate the spectral functions with a delta, $\mathcal{A}_s(p) \simeq \delta(E_p^s - \mu)$, and we easily obtain $\Gamma \simeq \Gamma_0$ for $\mu > 0$ and

$$\Gamma \simeq \Gamma^{WDA} = \Gamma_0 \sqrt{E_0/E_F} = \Gamma_0(n_0/n) \quad \text{for } \mu < 0. \quad (6)$$

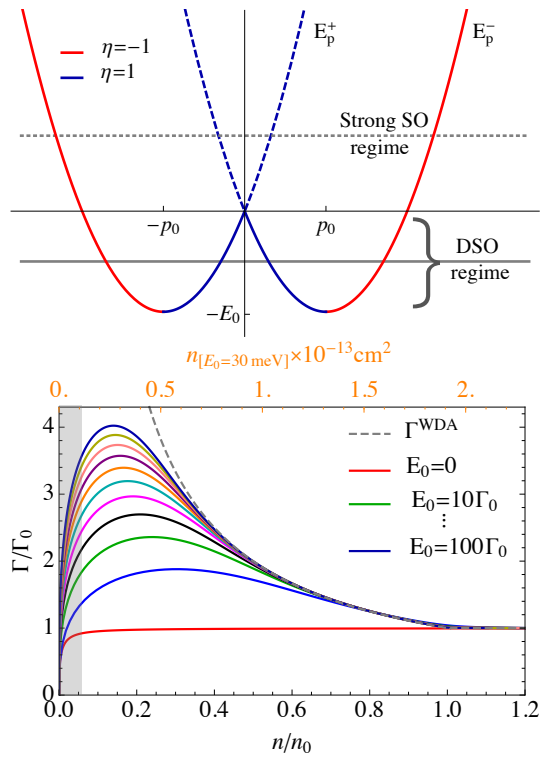


Figure 1: (Color online) (a) Band dispersion of the Rashba model. The red/blue color denote $\eta = \pm 1$ with $\eta = \text{sign}(\vec{v}_{\mathbf{p}s} \cdot \hat{p}) s$. (b) Scattering rate in units of $\Gamma_0 = 0.5\text{meV}$ as a function of n/n_0 for different E_0 (here we set $m = 0.7m_e$). The dashed line shows the WDA result Γ^{WDA} , Eq. (6). The upper x -axis scale displays the n corresponding to $E_0 = 35\text{meV}$. In the shaded region corrections beyond BA become important.

In the same WDA the electronic density, n , is given by the non-interacting result Eq.(3). In Fig.1b we plot the numerical self-consistent Γ as a function of the ratio n/n_0 for different values of the SO coupling and we compare it with its WDA approximation. As expected, the universal approximate curve given by the r.h.s. of Eq.(6) is accurate for large n/n_0 and its accuracy increases with increasing E_0/Γ_0 . On the contrary, as μ approaches the band edge, the DOS singularity is smeared by disorder and finite-band effects cut-off the divergence of the WDA result (6). In the extreme diluted limit, (shaded region in Fig.1b) Γ as given by the SCBA vanishes and higher-order corrections become important [53].

Let us now consider dc transport. Within linear response theory and SCBA, the static longitudinal conductivity $\sigma_{dc} \equiv \sigma_{xx}$ is given by [52]

$$\sigma_{dc} = \frac{1}{2\pi} (P_{xx}^{AR} - \text{Re}[P_{xx}^{RR}]) \quad (7)$$

with P_{xx}^{LM} denoting the current response function

$$P_{xx}^{LM} = \frac{1}{\mathcal{V}} \sum_{\mathbf{p}} \text{Tr} [j_x(\mathbf{p}) G^L(\mathbf{p}, 0) J_x^{LM}(\mathbf{p}) G^M(\mathbf{p}, 0)] \quad (8)$$

where the superscript $L, M = A, R$ indicate advanced/retarded arguments and $j^x(\mathbf{p})$ and $J_{LM}^x(\mathbf{p})$ denote respectively the bare and renormalized currents along x , i.e. $j_x(\mathbf{p}) \equiv ev_x(\mathbf{p}) = e(p_x/m + \alpha\sigma_y)$, while, within SCBA, the LM dressed current satisfies the following equation:

$$J_{LM}^x(\mathbf{p}) = j^x(\mathbf{p}) + n_i v_0^2 \sum_{\mathbf{k}} G^L(\mathbf{k}, 0) J_{LM}^x(\mathbf{k}) G^M(\mathbf{k}, 0). \quad (9)$$

Here the last term is momentum independent and, by symmetry arguments, it can be shown to be proportional to σ_y . The solution of Eq.(9) can be therefore written as,

$$J_{LM}^x(\mathbf{p}) \equiv eV_x^{LM} = e(p_x/m + \tilde{\alpha}^{LM}\sigma_y). \quad (10)$$

The renormalized anomalous vertex, $\tilde{\alpha}^{LM}$, that can be expressed in terms of G^L and G^M using Eq. (9) [53], has been widely discussed in the context of the spin-Hall effect [2, 45–47, 51]. In particular, for $\mu > 0$ vertex corrections cancel out [45, 46, 49] the anomalous contribution to the current yielding $\tilde{\alpha}_{RA}^{RA} = 0$, while for $\mu < 0$ one gets $\tilde{\alpha}_{RA} \neq 0$ [47]. In both cases the spin-Hall current is bound to be zero by symmetry arguments [46], so the effects of the anomalous current vertex are not visible in the spin-Hall effect. In contrast, as we show here, the persistence of the anomalous velocity term has crucial effects on the dc conductivity in the DSO regime.

In the chiral basis the current response function can be cast as the sum of an inter- and an intra-band term, i.e. $P_{xx}^{LM} = P_{\text{intra}}^{LM} + P_{\text{inter}}^{LM}$, with P_{intra}^{LM} and P_{inter}^{LM} respectively given by

$$P_{\text{intra}}^{LM} = \frac{e^2}{2V} \sum_{\mathbf{ps}} \vec{v}_{\mathbf{ps}} \cdot \vec{V}_{\mathbf{ps}}^{LM} g_s^L(p, 0) g_s^M(p, 0) \quad (11)$$

$$P_{\text{inter}}^{LM} = \frac{e^2}{2V} \alpha \tilde{\alpha}^{LM} \sum_{\mathbf{p} s \neq s'} g_s^L(p, 0) g_{s'}^M(p, 0). \quad (12)$$

where $\vec{v}_{\mathbf{ps}} = \mathbf{p}/m + s\alpha\hat{p}$ and $\vec{V}_{\mathbf{ps}}^{LM} = \mathbf{p}/m + s\tilde{\alpha}^{LM}\hat{p}$ are the diagonal components of the bare and renormalized velocity operators in the chiral basis. By means of Eqs. (11-12), along with the self-consistent self-energy and vertex equations (Eq. (9)), we calculate the static longitudinal conductivity for arbitrary values of the the SO coupling. The results are shown in Fig. 2(a-c), where we plot the conductivity (a,b) and the mobility $\mu_t = \sigma_{dc}/(e\hbar n)$ (c) as a function of the electronic density for different values of the SO coupling. As the system enters the DSO regime $n \leq n_0$ the conductivity, plotted in Fig.2(a), becomes sublinear, while the mobility is strongly reduced and it becomes density-dependent, as shown by Fig. 2(c). Furthermore, by appropriate rescaling σ_{dc} by $\sigma_{n_0} \equiv e^2 n_0 \tau_0 / (2m)$, all conductivity and mobility curves collapse on the dashed universal lines representing σ_{DSO} (from Eq. (1)) and $\mu_{DSO} \equiv \sigma_{DSO}/n$ in Fig.2b and Fig.2c, respectively. These analytical expressions can be derived by computing (7) in the WDA, where we can neglect the RR current response function, which

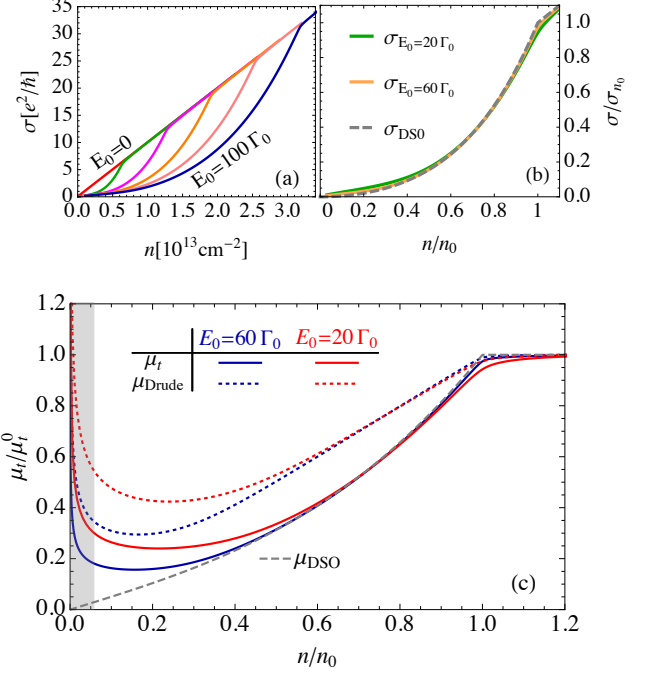


Figure 2: (Color online) (a) Conductivity versus electron density for $E_0 = 0, \dots, 100\Gamma_0$. (b) Universal behavior of the conductivity rescaled to σ_{n_0} . (c) Mobility μ_t normalized to $\mu_t^0 = e/(2\hbar\Gamma_0 m) \simeq 1475 \text{ cm}^2/(\text{V}\cdot\text{s})$, compared with different approximations, see text.

is of higher order in Γ/E_F [52, 53], and we can discard the interband term P_{inter}^{RA} in Eq. (12), due to the negligible overlap between the spectral functions of the two chiral bands [53]. The dc conductivity can be then simply recast as

$$\sigma_{dc} = \frac{e^2}{4V\Gamma} \sum_{\mathbf{ps}} \vec{v}_{\mathbf{ps}} \cdot \vec{V}_{\mathbf{ps}}^{RA} \delta(E_p^s - \mu), \quad (13)$$

where the anomalous vertex entering the dressed velocity $\vec{V}_{\mathbf{ps}}^{RA}$ leads to, in the WDA, $\tilde{\alpha}^{RA} = -2\mu/p_0$ for $\mu < 0$ [53]. By expressing the momenta of the electrons on the inner and outer Fermi circle, p_{\pm} , as follows

$$p_{\pm}^{\mu>0} = mv_F \mp p_0 \quad \text{and} \quad p_{\pm}^{\mu<0} = p_0 \mp mv_F. \quad (14)$$

with $v_F = \sqrt{2mE_F}$, after some algebra Eq. (13) reads

$$\sigma_{dc} \simeq \sigma_{\text{Drude}}^0 = ne^2\tau_0/m \quad \mu > 0 \quad (15)$$

$$\sigma_{dc} \simeq \sigma_{\text{Drude}}^{WDA} [1 + \mu/(2E_0)] = \sigma_{DSO} \quad \mu < 0 \quad (16)$$

where $\sigma_{\text{Drude}}^{WDA} = e^2 n / (2\Gamma^{WDA} m)$ denotes the Drude conductivity computed with the WDA approximation (6) of the scattering rate. By using Eqs.(3-6) to express μ and Γ^{WDA} as a function of n one eventually sees that Eq.(16) reduces to Eq.(1) above. We remark that the second term in square brackets in Eq.(16) is due to the anomalous vertex, i.e. σ_{DSO} can be expressed in terms of $\tilde{\alpha}_{RA}$

as $\sigma_{DSO} = \sigma_{\text{Drude}}^{WDA}[1 - \tilde{\alpha}_{RA}/(2\alpha)]$. Therefore the inclusion of vertex corrections is crucial to obtain the correct conductivity: the bare-bubble result, obtained by setting $\tilde{\alpha}^{RA} = \alpha$ in Eq. (13), simply yields $\sigma_{dc} \simeq \sigma_{\text{Drude}}^{WDA}/2$ at $\mu < 0$. Note that the bare-bubble result also fails at $\mu > 0$, where it gives $\sigma_{dc} \simeq \sigma_{\text{Drude}}^0 - \sigma_{n_0}$.

The accuracy of σ_{DSO} to reproduce the quantum results, and the deviations from Drude's law, emerge quite clearly in the mobility plotted in Fig. 2c. Here we also show for completeness the Drude mobility $\mu_{\text{Drude}} \equiv e^2/(2\Gamma m)$, computed with the full self-consistent scattering time Γ . As one can see, even accounting for the enhancement of the scattering rate, μ_{Drude} fails both qualitatively and quantitatively in the DSO regime. Indeed, even for densities where $\Gamma \simeq \Gamma^{WDA}$, the Drude formula does not account for the additional suppression of the conductivity due to the anomalous vertex, i.e. the factor in brackets in Eq. (16). The deviations of μ_{DSO} from μ_{Drude} at low density are due instead to two factors: (i) the deviations of Γ from Γ^{WDA} , shown in Fig. 1b, and (ii) the relevance of RR terms in Eq. (7) [53]. Finally, we remark that the divergence of the fully self-consistent mobility μ_{tr} in the extreme diluted limit, $n \lesssim 0.05$, (shaded region in Fig. 2c), is related to the vanishing of Γ within SCBA, and it must be disregarded.

Equation (13) is strongly reminiscent of the one usually found in the semiclassical Boltzmann approach [54], where the difference between the moduli of the bare velocity $v_{ps} = |\vec{v}_{\mathbf{p}s}|$ and of the dressed current $J_{p,s} \equiv e(\tau_{ps}^{tr}/\tau)v_{ps}$ in each band is usually rephrased in terms of a transport τ_{ps}^{tr} scattering time that in general differs from the quasiparticle scattering time τ . Boltzmann conductivity is then given by [54]

$$\sigma_{dc}^B = \frac{e^2}{2V} \sum_{\mathbf{p}s} \delta(\mu - E_p^s) v_{sp}^2 \tau_{ps}^{tr}. \quad (17)$$

Following the route outlined e.g in Ref.[54], τ_{ps}^{tr} can be shown to fulfill the following set of equations

$$\frac{\tau_{sp}^{tr}}{\tau} = 1 + \frac{n_i}{V} \sum_{\mathbf{k}'\beta} W_{\mathbf{p}\mathbf{p}'}^{ss'} \frac{\vec{v}_{\mathbf{p}'s'} \cdot \vec{v}_{\mathbf{p}s}}{|\vec{v}_{\mathbf{p}s}|^2} \tau_{s'p'}^{tr}. \quad (18)$$

Here $\tau^{-1} = n_i/V \sum_{ks} W_{\mathbf{p}\mathbf{p}'}^{ss'}$ is band independent and the collision integral $W_{\mathbf{p}\mathbf{p}'}^{ss'}$ is defined as $W_{\mathbf{p}\mathbf{p}'}^{ss'} = \pi v_{imp}^2 (1 + ss' \hat{p} \cdot \hat{p}') \delta(E_p^s - E_{p'}^{s'})$. The momentum dependence of τ_{sp}^{tr} is due to the chiral nature of the quasiparticle eigenstates of the Rashba model [49, 50]. In particular, if one defines the quantity $\eta = (\hat{v}_{\mathbf{p}s} \cdot \hat{p}) s$ one sees that, regardless the value of μ , the backscattering between states with the same η value is suppressed, see Fig.1, leading to a difference between the transport scattering times τ_{\pm} evaluated on the inner/outer Fermi circle. Solving Eq. (18) one easily finds that $1/(2\tau)$ coincides with Γ^{WDA} , while the

transport scattering times are given by:

$$\begin{cases} \tau_{\pm} = \tau p_{\pm}/p_0 & \mu < 0, \\ \tau_{\pm} = \tau p_{\pm}/(mv_F) & \mu > 0. \end{cases} \quad (19)$$

We then see that at $\mu > 0$ the renormalized Boltzmann currents on the inner and outer Fermi circles J_{\pm}^B coincide with the quantum renormalized currents, i.e. we get $J_{\pm}^B = J_{\pm}^{RA} = ep_{\pm}/m$ and $J_{\pm}^{RA} = eV_{\pm}^{RA}$ where the \pm subscripts refer to the quantities evaluated on the inner and outer Fermi circles (see Eq.(14)). At $\mu > 0$, where $\tilde{\alpha}^{RA} = 0$, one can indeed prove [50] that equations (18) are equivalent to the self-consistent vertex equation (9). This equivalence cannot be straightforwardly extended to the case $\mu < 0$. Indeed, as soon as the anomalous velocity term $\tilde{\alpha}^{RA}$ in Eq.(9) becomes finite, the renormalized current operator J^{RA} is no more diagonal in the chiral basis contrary to what assumed by standard semiclassical Boltzmann approach. As a result for $\mu < 0$, the quantum solution gives $J_{\pm}^{RA} = \mp(p_{\pm}/m - \alpha\mu/E_0)$ while the Boltzmann solution is $J_{\pm}^B = p_{\pm}/p_0$. Surprisingly, these differences cancel out when computing the conductivity so that, by simple algebra from Eqs.(17) and (19) we eventually get $\sigma_{dc}^B = \sigma_{DSO}$. Notice that a similar unexpected accuracy of Boltzmann approach for the conductivity has been also found in graphene, where again the velocity operator is not diagonal in the chiral basis [55]. It is of course not guaranteed that the same holds for other quantities involving different powers of the renormalized current, like e.g. the Hall resistance [56], as already observed in other multiband systems [57].

In conclusion, we have shown that SO coupling affects transport in a strongly density-dependent way causing significant deviations from Drude laws at low densities. These results may be relevant to understand the transport anomalies observed in LAO/STO interface [31–34] at low densities. The results of Fig. 1-2 have been obtained for $m = 0.7m_e$, as appropriate for the lower “lighter” band of SrTiO₃ and the used scattering rate ($\Gamma_0 = 0.5\text{meV}$) reproduces the mobility of LAO/STO in the high-doping limits, see e.g. Ref.[31]. These values also lead to $n_0 = 0.063 10^{13}\text{cm}^{-2} \times E_0[\text{meV}]$ and $\alpha = \sqrt{2E_0[\text{meV}]} \times 10^{-11}\text{eV m}$. By looking at Fig. 2b, we then see that for a SO coupling $\alpha \sim 6 \times 10^{-11}\text{eV m}$ one finds a suppression of the mobility by a factor of five in the same range of densities ($n \sim 1 \times 10^{13}$) where it is experimentally observed[31]. Even though this value of α is on the upper bound of the ones currently quoted in the literature[34, 58, 59], one should consider that such estimates rely on weak-localization fits done with formulas appropriate for the weak SO regime. Thus, the interpretation of existing transport data within a DSO scenario would also require an extension of the present theoretical results to include the effects of a longitudinal[33] and transverse[31, 34] magnetic field, and weak-localization effects. These open questions provide an interesting

framework for future developments in materials with strong Rashba interactions.

Acknowledgements We gratefully acknowledge fruitful discussions with S. Caprara, C. Castellani, M. Grilli and R. Raimondi. We acknowledge financial support by Italian MIUR under projects FIRB-HybridNanoDev-RBFR1236VV, PRIN-RIDEIRON-2012X3YFZ2, and Premiali-2012 AB-NANOTECH.

[1] R. Winkler, *Spin-Orbit Coupling Effects in Two-Dimensional Electron and Hole Systems* (Springer, Berlin-Heidelberg, 2003).

[2] G. Vignale, J. Supercond. Nov. Magn. **23**, 3 (2009).

[3] D. Berciou and P. Lucignano, arxiv: 1502.00570 (2015).

[4] A. A. Burkov, Phys. Rev. B **70**, 155308 (2004).

[5] R. Hanson, J. R. Petta, S. Tarucha, and L. M. K. Vandersypen, Rev. Mod. Phys. **79**, 1217 (2007).

[6] Y. Araki, G. Khalsa, and A. H. MacDonald, Phys. Rev. B **90**, 125309 (2014).

[7] E. M. Hankiewicz and G. Vignale, J. Phys.: Cond. Matter **21**, 253202 (2009).

[8] V. Broso, M. Jerger, P. San-Jos, G. Zarand, A. Shnirman, and G. Schön Phys. Rev. B **82**, 041309(R) (2010)

[9] A. Shnirman and I. Martin, Europhys. Lett. **78**, 27001 (2007).

[10] B. Bernevig, J. Orenstein, and S.-C. Zhang, Phys. Rev. Lett. **97**, 236601 (2006).

[11] M. Koenig, H. Buhmann, L. W. Molenkamp, T. Hughes, C.-X. Liu, X.-L. Qi, and S.-C. Zhang, J. Phys. Soc. Jpn. **77**, 031007 (2008).

[12] A. Y. Kitaev, Physics-Uspekhi **44**, 131 (2001).

[13] C. Nayak, A. Stern, M. Freedman, and S. Das Sarma, Rev. Mod. Phys. **80**, 1083 (2008).

[14] D. D. Awschalom and M. E. Flatte', Nat. Phys. **3**, 153 (2007).

[15] C. Ast, J. Henk, A. Ernst, L. Moreschini, M. Falub, D. Pacile', P. Bruno, K. Kern, and M. Grioni, Phys. Rev. Lett. **98**, 186807 (2007).

[16] C. Ast, D. Pacile', L. Moreschini, M. Falub, M. Papagno, K. Kern, M. Grioni, J. Henk, A. Ernst, S. Ostanin, and et al., Phys. Rev. B **77**, 081407 (2008).

[17] I. Gierz, T. Suzuki, E. Frantzeskakis, S. Pons, S. Ostanin, A. Ernst, J. Henk, M. Grioni, K. Kern, and C. R. Ast, Phys. Rev. Lett. **103**, 046803 (2009).

[18] H. Mirhosseini, A. Ernst, S. Ostanin, and J. Henk, J. Phys.: Condens. Matter **22**, 385501 (2010).

[19] K. Yaji, Y. Ohtsubo, S. Hatta, H. Okuyama, K. Miyamoto, T. Okuda, A. Kimura, H. Namatame, M. Taniguchi, and T. Aruga, Nature Comm. **1**, 17 (2010).

[20] D. V. Gruznev, L. V. Bondarenko, A. V. Matetskiy, A. A. Yakovlev, A. Y. Tupchaya, S. V. Eremeev, E. V. Chulkov, J.-P. Chou, C.-M. Wei, M.-Y. Lai, and et al., Sci. Rep. **4**, 4742 (2014).

[21] S. V. Eremeev, I. A. Nechaev, Y. M. Koroteev, P. M. Echenique, and E. V. Chulkov, Phys. Rev. Lett. **108**, 246802 (2012).

[22] M. Bahramy, B.-J. Yang, R. Arita, and N. Nagaosa, Nature Comm. **3**, 679 (2012).

[23] M. Sakano, M. Bahramy, A. Katayama, T. Shimojima, H. Murakawa, Y. Kaneko, W. Malaeb, S. Shin, K. Ono, H. Kumigashira, and et al., Phys. Rev. Lett. **110**, 107204 (2013).

[24] X. Xi, C. Ma, Z. Liu, Z. Chen, W. Ku, H. Berger, C. Martin, D. B. Tanner, and G. L. Carr, Phys. Rev. Lett. **111**, 155701 (2013).

[25] Y. Gui, C. Becker, N. Dai, J. Liu, Z. Qiu, E. Novik, M. Schaefer, X. Shu, J. Chu, H. Buhmann, and et al., Phys. Rev. B **70**, 115328 (2004).

[26] A. Ohtomo and H. Y. Hwang, Nature **427**, 423 (2004).

[27] S. Thiel, Science **313**, 1942 (2006).

[28] N. Reyren, S. Thiel, A. D. Caviglia, L. F. Kourkoutis, G. Hammerl, C. Richter, C. W. Schneider, T. Kopp, A.-S. Ruetschi, D. Jaccard, and et al., Science **317**, 1196 (2007).

[29] A. D. Caviglia, S. Gariglio, N. Reyren, D. Jaccard, T. Schneider, M. Gabay, S. Thiel, G. Hammerl, J. Mannhart, and J.-M. Triscone, Nature **456**, 624?627 (2008).

[30] C. Bell, S. Harashima, Y. Kozuka, M. Kim, B. G. Kim, Y. Hikita, and H. Y. Hwang, Phys. Rev. Lett. **103**, 226802 (2009).

[31] J. Biscaras, N. Bergeal, S. Hurand, C. Grossette, A. Rastogi, R. C. Budhani, D. LeBoeuf, C. Proust, and J. Lesueur, Phys. Rev. Lett. **108**, 247004 (2012).

[32] S. Seri, M. Schultz, and L. Klein, Phys. Rev. B **86**, 085118 (2012).

[33] M. Ben Shalom, M. Sachs, D. Rakhmievitch, A. Palevski, and Y. Dagan, Phys. Rev. Lett. **104**, 126802 (2010).

[34] A. D. Caviglia, M. Gabay, S. Gariglio, N. Reyren, C. Cancellieri, and J.-M. Triscone, Phys. Rev. Lett. **104**, 126803 (2010).

[35] A. Joshua, J. Ruhman, S. Pecker, E. Altman, and S. Ilani, Proc. Nat. Acad. Sci. **110**, 9633 (2013).

[36] Q. Liu, Y. Guo, and A. J. Freeman, Nano Lett. **13**, 5264 (2013).

[37] J. Biscaras, S. Hurand, C. Feuillet-Palma, A. Rastogi, R. C. Budhani, N. Reyren, E. Lesne, J. Lesueur, and N. Bergeal, Sci. Rep. **4**, 6788 (2014).

[38] Z. Zhong, L. Si, Q. Zhang, W.-G. Yin, S. Yunoki, and K. Held, Adv. Mater. Interfaces **2**, 201400445 (2015).

[39] E. I. R. Y. A Bychkov, JETP Letters **39**, 66 (1984).

[40] J. A. Sulpizio, S. Ilani, P. Irvin, and J. Levy, Annu. Rev. Mater. Res. **44**, 117 (2014).

[41] E. I. Rashba, Phys. Rev. B **86**, 125319 (2012).

[42] A. Chaplik and L. Magarill, Phys. Rev. Lett. **96**, 126402 (2006).

[43] C. Grimaldi, Phys. Rev. B **72**, 075307 (2005).

[44] E. Cappelluti, C. Grimaldi, and F. Marsiglio, Phys. Rev. Lett. **98**, 167002 (2007).

[45] R. Raimondi and P. Schwab, Phys. Rev. B **71**, 033311 (2005).

[46] O. Dimitrova, Phys. Rev. B **71**, 245327 (2005).

[47] C. Grimaldi, E. Cappelluti, and F. Marsiglio, Phys. Rev. B **73**, 081303 (2006).

[48] E. M. Hankiewicz and G. Vignale Phys. Rev. Lett. **100**, 026602 (2008)

[49] R. Raimondi, M. Leadbeater, P. Schwab, E. Caroti, and C. Castellani, Phys. Rev. B **64**, 235110 (2001).

[50] P. Schwab and R. Raimondi, Eur. Phys. J. B **25**, 483 (2002).

[51] R. Raimondi, P. Schwab, C. Gorini, and G. Vignale, Annalen der Physik **524**, 153 (2011).

- [52] G. D. Mahan, *Many-Particle Physics* (Springer, Berlin-Heidelberg, 2000).
- [53] See Supplementary Material for more details.
- [54] J. M. Ziman, *Principles of the Theory of Solids* (Cambridge University Press, Cambridge, United Kingdom, 1972).
- [55] E. Cappelluti and L. Benfatto, Phys. Rev. B **79**, 035419 (2009).
- [56] H. Fukuyama, H. Ebisawa, and Y. Wada, Progr. of Theoretical Phys. **42**, 494 (1969).
- [57] L. Fanfarillo, E. Cappelluti, C. Castellani, and L. Benfatto, Phys. Rev. Lett. **109**, 096402 (2012).
- [58] A. Fête, C. Cancellieri, D. Li, D. Stornaiuolo, A. D. Caviglia, S. Gariglio, and J.-M. Triscone, Appl. Phys. Lett. **106**, 051604 (2015).
- [59] M. Diez, A. M. R. V. L. Monteiro, G. Mattoni, E. Cobanera, T. Hyart, E. Mulazimoglu, N. Bovenzi, C. W. J. Beenakker, and A. D. Caviglia, arXiv:1412.5614 (2014).